Proc. Natl. Acad. Sci. USA
Vol. 93, pp. 11913–11918, October 1996
Microbiology

Haemophilus influenzae pili are composite structures assembled via the HifB chaperone

(organelle biogenesis/pathogenesis)

JOSEPH W. ST. GEME III*†‡, JEROME S. PINKNER†, GRAHAM P. KRASAN*, JOHN HEUSER§, ESTHER BULLITT¶, ARNOLD L. SMITH‖, AND SCOTT J. HULTGREN†

*Edward Mallinckrodt Department of Pediatrics, and Departments of †Molecular Microbiology and §Cell Biology and Physiology, Washington University School of Medicine, St. Louis, MO 63110; ¶Department of Biophysics, Boston University School of Medicine, Boston, MA 02118; and ‖Department of Molecular Microbiology and Immunology, University of Missouri, Columbia, MO 65203

Communicated by Stanley Falkow, Stanford University School of Medicine, Stanford, CA, August 5, 1996 (received for review April 19, 1996)

ABSTRACT **_Haemophilus influenzae_ is a Gram-negative bacterium that represents a common cause of human disease. Disease due to this organism begins with colonization of the upper respiratory mucosa, a process facilitated by adhesive fibers called pili. In the present study, we investigated the structure and assembly of _H. influenzae_ pili. Examination of pili by electron microscopy using quick-freeze, deep-etch and immunogold techniques revealed the presence of two distinct subassemblies, including a flexible two-stranded helical rod comprised of HifA and a short, thin, distal tip structure containing HifD. Genetic and biochemical studies demonstrated that the biogenesis of _H. influenzae_ pili is dependent on a periplasmic chaperone called HifB, which belongs to the PapD family of immunoglobulin-like chaperones. HifB bound directly to HifA and HifD, forming HifB–HifA and HifB–HifD complexes, which were purified from periplasmic extracts by ion-exchange chromatography. Continued investigation of the biogenesis of _H. influenzae_ pili should provide general insights into organelle development and may suggest novel strategies for disease prevention.**

Mucosal colonization is an essential early step in the pathogenesis of most bacterial diseases (1). Bacterial attachment to host epithelial cells is a key event in this process and is mediated by specialized proteins called adhesins, which are usually components of hair-like surface fibers (2).

Among Gram-negative bacteria, adhesive fibers are most often assembled in a process that involves an immunoglobulin-like periplasmic chaperone and an outer membrane protein called an usher (2). Fibers assembled by the chaperone/usher pathway have diverse molecular architectures ranging from rod-like cylinders called pili to very thin flexible filaments that coil into an amorphous mass on the bacterial surface (3). At least some adhesive fibers are composite structures consisting of rod-like subassemblies joined distally to very thin fibrillae (tip fibrillae) (4, 5).

The prototype periplasmic chaperone is PapD, which is required for assembly of P pili in uropathogenic *Escherichia coli*. This protein has been shown to have an immunoglobulin-like three-dimensional structure and functions by preventing premature subunit assembly in the periplasm (6, 7). PapD binds to and caps interactive surfaces on subunits by forming chaperone–subunit complexes, which are then escorted to outer membrane assembly sites comprised of the PapC usher (7, 8). Subsequently, complexes are dissociated, and subunits are incorporated into pili across the outer membrane. In the absence of an interaction with PapD, pilus subunits misfold and form off-pathway aggregates that are proteolytically degraded (7).

The publication costs of this article were defrayed in part by page charge payment. This article must therefore be hereby marked "*advertisement*" in accordance with 18 U.S.C. §1734 solely to indicate this fact.

Haemophilus influenzae is a Gram-negative coccobacillus that represents a frequent etiology of both localized respiratory tract and systemic disease (9). Disease due to *H. influenzae* begins with colonization of the nasopharynx, followed by either contiguous spread within the respiratory tract or invasion of the bloodstream. In 1982 two groups reported the presence of pili on selected *H. influenzae* isolates (10, 11). These structures were found to promote attachment to human oropharyngeal epithelial cells and to mediate agglutination of human erythrocytes expressing the AnWj antigen (12). Several studies have demonstrated that pili enhance adherence to human nasopharyngeal and nasal turbinate tissue in organ culture (13–15). More recently, Weber *et al.* (16) observed that pili play an important role in colonization using the monkey nasopharyngeal colonization model.

Genetic evidence suggests that the biogenesis of *H. influenzae* pili depends on the chaperone/usher pathway. The gene cluster required for assembly of pili has been cloned and includes a gene designated *hifA*, which encodes the major structural subunit (HifA) of the pilus (17). The remainder of the cluster is located upstream of *hifA* and is transcribed divergently, beginning with a chaperone-like gene designated *hifB*, followed by an usher-like gene, *hifC*, and then two genes with unknown functions, *hifD* and *hifE* (17–20). A detailed analysis of the architecture of *H. influenzae* pili has been lacking. Similarly, little information exists regarding the protein–protein interactions involved in the biogenesis of these appendages. The present study was undertaken to investigate the structure and assembly of *H. influenzae* pili.

MATERIALS AND METHODS

Bacterial Strains and Plasmids. *H. influenzae* strain Eagan is a type b strain that was originally isolated from the cerebrospinal fluid of a child with meningitis. The nucleotide sequences of the *hifA-E* genes in this strain have been reported (refs. 19–21; A.L.S., unpublished work). *E. coli* strains DH5α, ORN103, and C600 have been previously described (22, 23).

Plasmid pMCC10 contains the *hifA* and *hifB* genes and the 5′ portion of the *hifC* gene from strain Eagan. Plasmid pABK15 is a derivative of pMCC10 with the kanamycin cassette from pUC4K (24) inserted at the *Xho*I site within *hifB*. Plasmid pDC101 is also a derivative of pMCC10 and contains a kanamycin cassette inserted at the *Eco*RI site within *hifC*. Plasmid pJS201 contains *hifA* by itself downstream of the *trc* promoter in pTrc99A. The *hifA* gene was amplified from pABK15 using the polymerase chain reaction (PCR) and primers that correspond to nucleotides 73–92 bases upstream

Abbreviations: IPTG, isopropyl β-D-thiogalactoside; FPLC, fast protein liquid chromatography.

‡To whom reprint requests should be addressed at: Department of Molecular Microbiology, Washington University School of Medicine, 660 South Euclid Avenue, Box 8230, St. Louis, MO 63110. e-mail: stgeme@borcim.wustl.edu.

of the *hifA* start codon and 34–54 bases downstream of the stop codon. Plasmid pJS202 contains *hifB* by itself downstream of the *tac* promoter in pMMB91. The *hifB* gene was amplified from strain Eagan chromosomal DNA using the PCR and primers corresponding to sequences 53–72 nt upstream of the start codon and 27–46 nt downstream of the stop codon. Plasmid pGK101 contains *hifD* by itself downstream of the *trc* promoter in pTrc99A. The *hifD* gene was amplified from Eagan chromosomal DNA using the PCR and primers that correspond to the 5′ end and 3 bases upstream and the 3′ end and 3 bases downstream of *hifD*.

Purification of *H. influenzae* Pili. To purify pili from *H. influenzae* strain Eagan, bacteria were incubated in supplemented brain heart infusion broth (25) at 37°C overnight. Cells were then centrifuged at 8000 × *g* at 4°C for 20 min and were resuspended in 0.1 M Tris buffer (pH 8). Pili were sheared from the cell surface by blending at low speed for 10 min in an Omnimixer (Omni International, Waterbury, CT) immersed in ice. Following centrifugation at 25,000 × *g* at 4°C for 60 min, the supernatant was recovered and precipitated with 10% saturated ammonium sulfate. The resulting solution was centrifuged at 15,000 × *g* at 4°C for 20 min, and the supernatant was then precipitated with 45% saturated ammonium sulfate. Precipitation was repeated with 10% and then 45% saturated ammonium sulfate, and the final pilus pellet was resuspended in 0.5 M Tris (pH 7).

Purification of HifB, HifB–HifA Complex, and HifB–HifD Complex. HifB was purified from *E. coli* C600 carrying pJS202 (*hifB*). Bacteria were grown in 20 liters of Luria–Bertani broth to an optical density at 600 nm of 1.0 and were then induced with 0.25 mM isopropyl β-D-thiogalactoside (IPTG) for 1 h. Subsequently periplasmic proteins were extracted, concentrated with 75% saturated ammonium sulfate, and dialyzed against 20 mM Mes (pH 6.5). The resulting material was fractionated on a fast protein liquid chromatography (FPLC) HiLoad S Sepharose cation exchange column and eluted with a gradient of 0 to 1 M KCl. The fractions containing HifB were pooled and dialyzed against 50 mM phosphate, pH 7.0/1 M ammonium sulfate and then fractionated on an FPLC phenyl superose hydrophobic interaction column.

HifB–HifA complex was purified from strain C600 carrying pJS201 (*hifA*) and pJS202 (*hifB*). Bacteria were grown and induced as described in the previous paragraph. Following induction, periplasmic proteins were extracted, concentrated with 75% saturated ammonium sulfate, dialyzed against 20 mM Tris (pH 7.5), and then collected as flow-through on an FPLC HiLoad Q Sepharose anion exchange colum. The fractions containing HifB–HifA complex were pooled and dialyzed against 20 mM Mes (pH 6.5). The resulting sample was then fractionated on an FPLC HiLoad S Sepharose cation exchange column, eluting with a gradient of 0 to 1 M KCl.

HifB–HifD complex was purified from strain C600 harboring pGK101 (*hifD*) and pJS202 (*hifB*) using the protocol described for HifB–HifA complex.

Electron Microscopy. *Freeze etch.* Purified pili were prepared for electron microscopy by adsorption to mica chips which were quick-frozen, then freeze-fractured and deep-etched, and finally rotary replicated with platinum (26, 27). Whole bacteria were prepared for examination by incubating in supplemented brain heart infusion broth to log phase and then washing once with phosphate-buffered saline (PBS). Subsequently bacteria were adsorbed to glass coverslips which were quick-frozen, completely freeze-dried, and then rotary replicated with platinum (27).

Negative staining. Bacteria were grown on chocolate agar plates for ≈20 h, then suspended in PBS, and negatively stained with 0.5% uranyl acetate as described (25). Protein preparations were diluted to a concentration of ≈10 μg/ml, then spotted onto carbon-coated 300 mesh copper grids, washed with eight drops of buffer, and stained with 2% uranyl acetate for 15 sec.

Immunolabeling. Bacteria were prepared for immunoelectron microscopy as described by Roberts *et al.* (28) with minor modifications. In brief, glow-discharged carbon-coated, formvar-strengthened grids were overturned on a drop of bacterial suspension and incubated for 2 min. Subsequently, samples were blocked for 1 h with PBS containing 23% goat serum and 0.1% gelatin and were then incubated for 2 h with a 1:25 dilution of primary antibody. Next, samples were washed with PBS and incubated for 1 h with a 1:25 dilution of goat anti-rabbit IgG conjugated to 12-nm colloidal gold beads (Jackson ImmunoResearch). Samples were then washed again with PBS, fixed with 1% glutaraldehyde in PBS, and negatively stained with 0.5% uranyl acetate.

Cell Fractionation and Protein Analysis. Whole-cell lysates were prepared by resuspending bacterial pellets in water and an equal volume of 2× Laemmli buffer (29). Periplasmic proteins were extracted from *H. influenzae* using polymyxin B sulfate, as described (30). Periplasmic proteins were recovered from *E. coli* derivatives according to the method of Slonim *et al.* (31). Proteins were resolved by SDS/PAGE using 10%-12.5% acrylamide gels (29). Western blots were performed with mouse ascites fluid AF100 raised against denatured HifA or rabbit antiserum raised against purified HifB, HifB–HifA complex, denatured HifD, or HifB–HifD complex. Denatured HifA was obtained by resolving purified pili on an SDS/polyacrylamide gel and excising the monomeric HifA band, while denatured HifD was prepared by resolving purified HifB–HifD complex by SDS/PAGE and excising the HifD band. The excised material was minced and then used to immunize animals.

Recombinant DNA Methods. DNA ligations, restriction endonuclease digestions, and gel electrophoresis were performed according to standard techniques (22). In *H. influenzae*, transformation was performed using the MIV method of Herriott *et al.* (32).

Construction of HifB⁻ and HifC⁻ Mutants. Mutagenesis of *hifB* involved transformation of strain Eagan with linearized pABK15, followed by selection with kanamycin. Similarly, insertional inactivation of *hifC* was accomplished by transforming strain Eagan with linearized pDC101 and selecting with kanamycin. Allelic exchange was confirmed by Southern hybridization, probing with the kanamycin cassette from pUC4K (24) and *hifB* or *hifC*, as appropriate.

RESULTS

***H. influenzae* Pili Are Composite Structures.** To assess the structural features of *H. influenzae* pili, purified pili from strain Eagan were examined by quick-freeze, deep-etch electron microscopy (Fig. 1). As shown in row 1 of Fig. 1, inspection at high magnification revealed a relatively thick rod and a short thin tip differentiation reminiscent of the tip fibrillum seen on P and type 1 pili (4, 5). Consistent with observations made by conventional electron microscopy, pilus rods displayed many bends and flexures, implying that they are flexible. A number of pilus tips were noted to form curved hooks, suggesting that these structures are flexible as well.

Close examination of replicas of pilus rods revealed a diameter of 8–10 nm; subtraction of platinum shadowing allowed the calculation of a true diameter of 6–7 nm. In addition, these structures were noted to have regularly spaced horizontal striations indicative of a tight helical architecture. Interestingly, a cross-over repeat, consistent with a two-stranded helical structure was observed. This cross-over repeat was best appreciated in fields with multiple fibers aligned alongside one another (Fig. 1, row 2). The single-start helix was determined to be left-handed with a repeat of 5.2 nm, while the double-start helix was found to be right-handed with a cross-over repeat of 26 nm. Using these repeat dimensions, pilus rods were calculated to have five subunits per double-start half-turn. Overall, *H. influenzae* pilus rods showed a striking

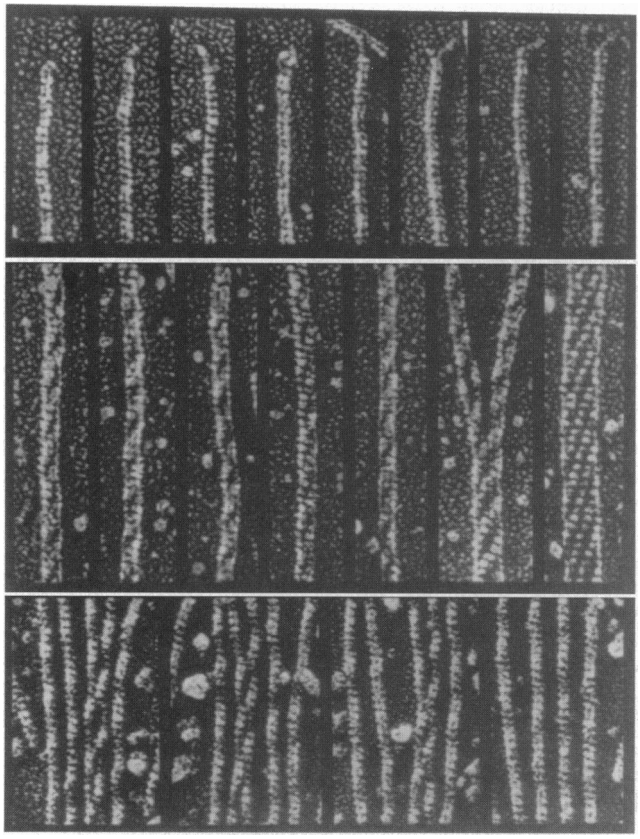

FIG. 1. Freeze-etch electron microscopy of purified pili and filamentous actin. Row 1 depicts the ends of purified pili from *H. influenzae* strain Eagan, highlighting very short tip differentiations. The closely spaced horizontal striations in the pilus rod are characteristic of a tight helix. Row 2 shows alignment of pili either two abreast (panels 1–4), four abreast (panel 5), or five abreast (panel 6); the bleed-over of the platinum coating between adjacent pili highlights the presence of a cross-over repeat, which is indicative of a two-stranded helical architecture. Row 3 depicts F-actin from rabbit skeletal muscle for comparison; note the striated appearance and cross-over repeat. Again the bleed-over of the platinum coating between actin filaments highlights the cross-over repeat. (×192,000.)

resemblance to filamentous actin (Fig. 1, row 3), which is known to be a two-stranded structure with actin monomers arranged in a single-start left-handed helix and a double-start right-handed helix.

Analysis of pilus tips revealed a diameter of ≈2.5 nm and an average length of roughly 16 nm. Based on examination of relatively straight tips, there was little variation in length from one tip to another.

Whole bacteria were also examined using the quick-freeze, deep-etch technique. The structures emanating from the surface of whole organisms had the same morphologic features as purified pili, including a striated appearance and a 26-nm cross-over repeat (not shown). Since a relatively low resolution protocol was required for these studies, it was difficult to resolve the presence of tip differentiations.

HifB Is a Periplasmic Chaperone That Stabilizes HifA. Given the apparent two-stranded architecture of *H. influenzae* pili, we wondered whether the general principles that govern the chaperone/usher assembly pathway would still apply. The *Haemophilus* pilus gene cluster includes a gene designated *hifB* which encodes a product (HifB) with homology to PapD (17). Molecular modeling has suggested that HifB is a member of the PapD family of immunoglobulin-like chaperones (6).

Using *E. coli* C600 harboring pJS202 (*hifB*), HifB was overexpressed and then purified from periplasmic extracts (see Fig. 3*A*, lane 1, and Fig. 6*A*, lane 6). N-terminal amino acid sequencing of the purified protein revealed the sequence -VIITGTGT, which corresponds to residues beginning at position 25 in the predicted HifB polypeptide. (The identity of the first residue could not be determined because of excessive background.) The cleaved 24-amino acid fragment has features of a typical prokaryotic signal peptide and terminates with the sequence ANA. Examination of purified HifB by isoelectric focusing demonstrated a pI of >9 (not shown), similar to that of PapD and other chaperones belonging to the PapD family. Cell fractionation studies performed with anti-HifB antiserum confirmed that in *H. influenzae* strain Eagan and in *E. coli* C600/pJS202, HifB was most abundant in the periplasm and was absent from the outer membrane (not shown).

Insertional inactivation of the *hifB* gene in *H. influenzae* strain Eagan eliminated expression of pili on the surface of the organism and abolished bacterial-mediated hemagglutination (not shown). As shown in Fig. 2*A*, examination of this strain by immunoblotting with anti-HifA antibody revealed no detectable HifA in either periplasmic extracts or whole cell lysates. In contrast, insertional inactivation of *hifC*, the downstream gene in the *hif* gene cluster, had no effect on the quantity of HifA in the periplasm or in whole cells (Fig. 2*A*). These results suggested that HifB serves to stabilize HifA against degradation. To pursue this consideration further, clones containing either *hifA* (pJS201) or *hifB* (pJS202) or both were introduced into *E. coli* ORN103. Following induction of gene expression with IPTG, periplasmic fractions were isolated from each of these strains and examined for reactivity with antibody against HifA. As shown in Fig. 2*B*, HifA could not be detected in *E. coli* harboring *hifA* alone but was easily visualized in *E. coli* carrying both *hifA* and *hifB*. *E. coli* harboring *hifB* alone failed to react with antibody against HifA.

HifB–HifA Complexes Are the Major Building Blocks of Pilus Rods. The observation that HifB functions to stabilize HifA suggested that these two proteins interact with one another

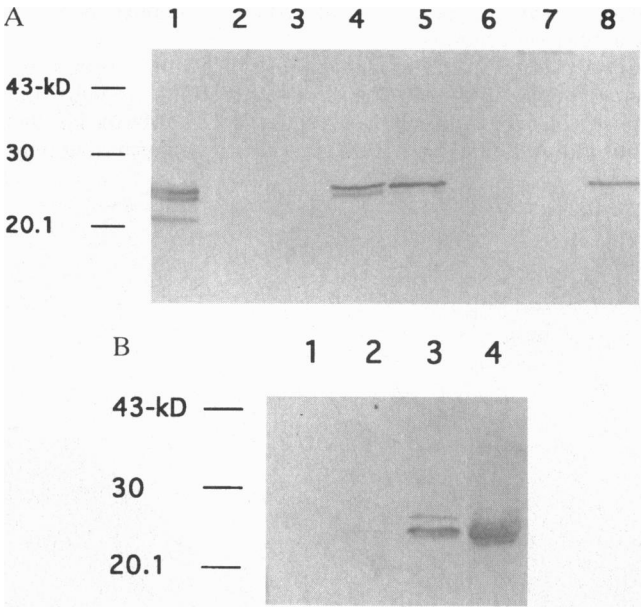

FIG. 2. Western analysis of *H. influenzae* strain Eagan and isogenic *hifB* and *hifC* mutants and of *E. coli* ORN103 carrying pJS201 (*hifA*), pJS202 (*hifB*), or both, blotting with anti-HifA antibody. (*A*) Whole-cell lysates and periplasms from strain Eagan derivatives. Lanes: 1, whole-cell lysate from piliated wild-type strain; 2, whole-cell lysate from nonpiliated phase variant; 3, whole-cell lysate from HifB mutant; 4, whole-cell lysate from HifC mutant; 5, periplasm from piliated wild-type strain; 6, periplasm from nonpiliated phase variant; 7, periplasm from HifB mutant; 8, periplasm from HifC mutant. (*B*) Periplasms from *E. coli* ORN103 derivatives. Lanes: 1, *E. coli* ORN103/pJS201; 2, *E. coli* ORN103/pJS202; 3, *E. coli* ORN103/pJS201 plus pJS202; 4, purified pili.

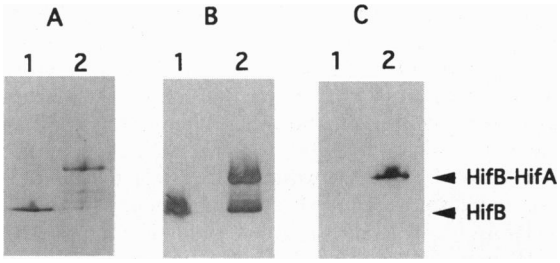

FIG. 3. Purification of HifB–HifA complex from periplasm of *E. coli* C600 carrying pJS201 (*hifA*) and pJS202 (*hifB*). Lanes: 1, purified HifB; 2, material purified from *E. coli* C600 (pJS201 plus pJS202). (*A*) Native polyacrylamide gel stained with Coomassie blue. (*B*) Native polyacrylamide gel examined by Western blot with antibody against HifB. (*C*) Native polyacrylamide gel examined by Western blot with antibody against HifA.

directly. To investigate this possibility, we attempted to demonstrate a HifB–HifA complex in the periplasmic fraction from *E. coli* C600 carrying pJS201 (*hifA*) and pJS202 (*hifB*). Periplasmic proteins from this strain were subjected to anion exchange chromatography, and fractions that contained both HifB and HifA were subsequently subjected to cation exchange chromatography. Analysis of the resulting material on a native polyacrylamide gel followed by staining with Coomassie blue revealed one predominant protein band and three minor bands (Fig. 3). The predominant band reacted with both anti-HifB and anti-HifA antibodies, indicating that this band represents a HifB–HifA complex. Of the three minor bands, one migrated to the same position as purified HifB and reacted only with anti-HifB antiserum, arguing that this band represents free HifB. The other two minor bands failed to react with either antibody preparation and are presumably contaminating proteins. Analysis of periplasmic extracts from strain Eagan by an analogous approach also demonstrated evidence of a HifB–HifA complex, although in smaller quantities (not shown).

Previous studies have suggested that HifA is the major structural subunit of the mature pilus. However, efforts to confirm this conclusion microscopically have been complicated by the fact that antiserum raised against HifA excised from a denaturing polyacrylamide gel fails to react with native pili (33). To circumvent this problem, we generated rabbit antiserum against purified HifB–HifA complex. Based on observations with PapD and P pilus subunits, we assumed that HifB holds HifA in a native conformation. The resulting antiserum was adsorbed with Eagan-*hifB*$^-$ to remove antibodies against contaminating proteins and was then used to examine piliated Eagan by immunoelectron microscopy. As shown in Fig. 4*A*, this antiserum decorated the entire shaft of the pilus. In contrast, anti-HifB antiserum failed to react with pili (Fig. 4*B*), arguing that the reactivity observed with the antiserum against HifB–HifA complex was due to antibodies against HifA. In control samples with Eagan*hifB*$^-$, there was no labeling with either the anti-HifB–HifA or the anti-HifB antiserum (not shown).

Chaperones are thought to control pilus assembly by capping and uncapping the associative surfaces of pilus subunits (7). In recent work, the major subassemblies of *E. coli* P pili, namely the pilus rod comprised of PapA and the tip fibrillum comprised of PapE, were reconstituted *in vitro* from purified chaperone-subunit complexes (42). Freeze–thaw techniques were used to achieve chaperone uncapping of PapA and PapE, resulting in the formation of pilus rods and tip fibrillae, respectively. To extend these observations, purified HifB–HifA complex was spotted onto carbon-coated grids, stained with uranyl acetate, and then examined by transmission electron microscopy. As shown in Fig. 5, numerous short rods were detected; these rods ranged in length from 10 to 100 nm and were virtually identical in appearance to mature *H. influenzae* pilus rods. The short rods presumably represent HifA multimers that formed after spontaneous dissociation of HifB from HifA.

HifB–HifD Complexes Are Precursors of Pilus Tips. The *hifD* gene is located immediately downstream of *hifC* and encodes a protein with homology to HifA (17, 20). Based on this homology and the presence of a chaperone binding motif at the carboxyl terminus, HifD is presumed to be a minor structural subunit (17, 20). To investigate this possibility, we began by constructing an *E. coli* C600 derivative harboring both *hifB* and *hifD* (pJS202 and pGK101). Following induction of gene expression with IPTG, periplasmic proteins were extracted and examined by SDS/PAGE. As shown in Fig. 6*A*, induced proteins corresponding in size to HifB (≈25 kDa) and HifD (21–22 kDa) were observed.

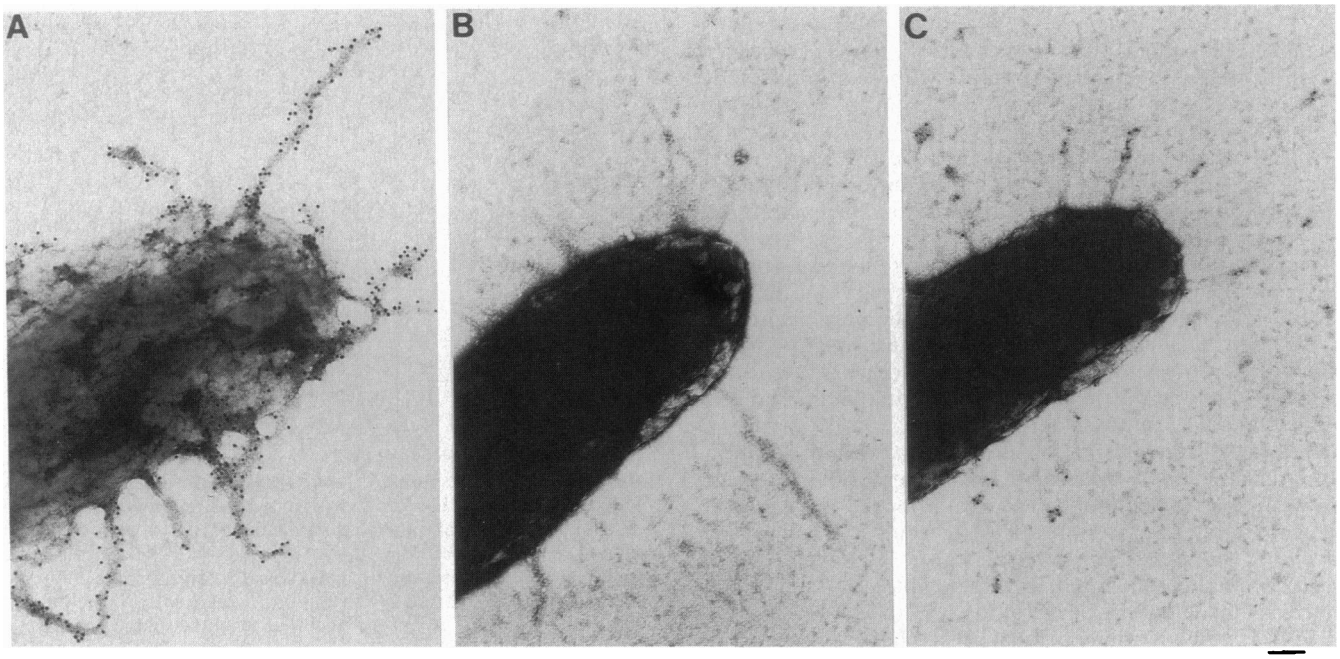

FIG. 4. Immunoelectron micrographs of *H. influenzae* strain Eagan. Samples were prepared with piliated strain Eagan and antisera against HifB–HifA complex (*A*), HifB (*B*), and HifB–HifD complex (*C*). (Bar = 110 nm.)

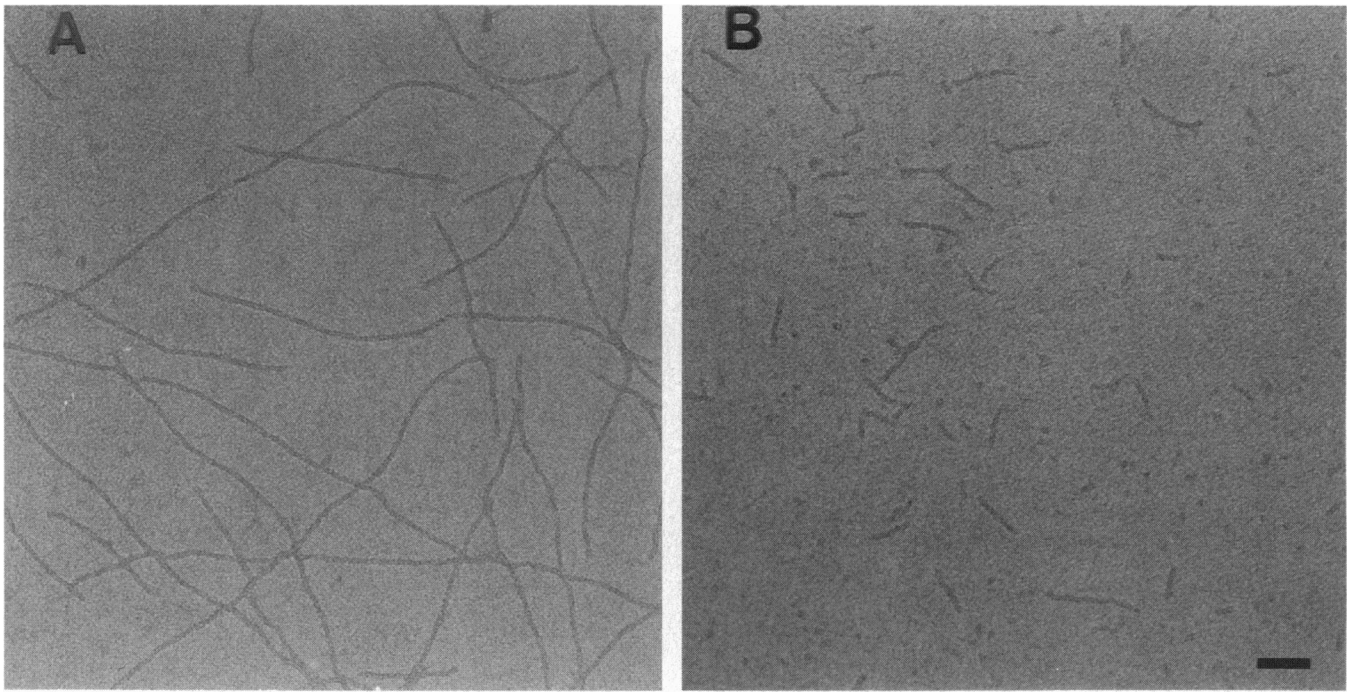

FIG. 5. Negatively stained electron micrographs of purified pili versus purified HifB–HifA. (*A*) Purified pili from *H. influenzae* strain Eagan. (*B*) Purified HifB–HifA; note that the short filaments are virtually identical in morphology to pure pili. (Bar = 50 nm.)

Using a scheme similar to that employed to purify HifB–HifA complex, we purified HifB–HifD complex by ion exchange chromatography (Fig. 6*A*). N-terminal amino acid determination revealed that mature HifD begins with the sequence VDGRVTFQGE, indicating cleavage of a 54-amino acid signal peptide that terminates with AYA.

In further experiments, HifB–HifD complex was loaded onto a preparative SDS/polyacrylamide gel, and the HifD band was excised and injected into rabbits. As shown in Fig. 6*B*, the resulting antiserum recognized HifD and also reacted with purified pili. In contrast, there was no reactivity with HifA (lane 6). Considered together, these findings indicate that HifD is incorporated into the mature pilus.

To localize HifD within the pilus structure, we generated antiserum against purified HifB–HifD complex and examined piliated Eagan by immunoelectron microscopy. As shown in Fig. 4*C*, gold beads were present predominantly at the ends of pili, suggesting that HifD is a component of the tip differentiation at the distal end of the pilus. In a control sample with Eagan*hifB*$^-$, we observed no labeling (not shown).

DISCUSSION

Quick-freeze deep-etch electron microscopy has been employed previously to examine P and S pili (4, 34), which are expressed exclusively by *E. coli*, and type 1 pili (5), which are common to members of the family Enterobacteriaceae. These fibers are composite structures consisting of a single-stranded helical rod that emanates from the bacterial surface and connects to a distally located tip fibrillum. P pilus and type 1 pilus rods have been characterized in detail, and their helical symmetry is known to be right-handed (35, 36). *H. influenzae* pili represent the first pilus organelles outside the family Enterobacteriaceae to be examined by high resolution electron microscopy. Our results indicate that *H. influenzae* pili are composite structures as well. However, their architecture is distinctive, with the pilus rod consisting of a single-start left-handed helix and a double-start right-handed helix.

In general, the molecular architecture of a pilus is determined by the structural properties and interactive surfaces of the subunits (42). Bullitt and Makowski (35) recently demonstrated that the P pilus rod is a thread-like PapA fibrillar polymer that is tightly wound to generate the mature helical rod. Each PapA subunit in the pilus makes at least two contacts that are described as head-to-tail. The tail of the subunit is defined in part by the conserved carboxy terminus of pilus subunits that is also recognized by the PapD chaperone (G. Soto and S.J.H., unpublished work). However, PapA subunits must make additional packaging interactions to transform the thin fibrillar conformation of the PapA polymer into the single-stranded right-handed helical structure. HifA subunits also contain the conserved carboxyl-terminal chaperone binding motif and are presumably held together in a head-to-tail fashion within each strand. In addition, the HifA subunits in each of the two left-handed helical strands must interact with subunits in the opposite strand to package into a double-start right-handed helix. In this respect, the interactive surfaces of HifA subunits may be more similar to those of actin monomers than to PapA or other pilus subunits.

Our results suggest that the *H. influenzae* pilus tip fibrillum contains the minor subunit called HifD. It is possible that the HifE protein, which is a putative second minor subunit and is encoded by the gene immediatedly downstream of *hifD* (17, 20), is also incorporated into the tip. HifE possesses a chaperone binding motif at the carboxyl terminus and shares homology with a number of minor pilus subunits (17, 20). In P pili and type 1 pili, the pilus tip contains the adhesive subunit responsible for binding to the relevant host cell receptor (4, 5). In this context, it is noteworthy that van Ham *et al.* (37) recently suggested that HifA represents the adhesive moiety in *H. influenzae* pili. These investigators based their conclusion on the observation that *E. coli* DH5α harboring the *hif* gene cluster with a kanamycin cassette in the *hifD* gene was capable of moderate attachment to human cells. The *hifD* insertion was believed to eliminate expression of both *hifD* and the downstream *hifE*, such that only HifA, HifB, and HifC were being synthesized. Our demonstration that *H. influenzae* pili contain tip fibrillae raises the possibility that a minor subunit localized to the tip is the true adhesin. Experiments to address this issue are presently in progress.

In previous studies, insertional inactivation of *hifD* resulted in a marked decrease in the number of pili (17, 20). An in-frame

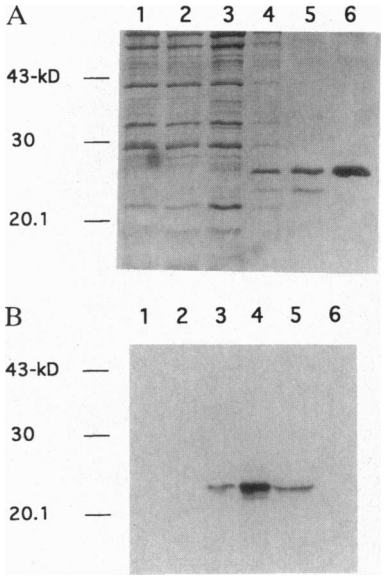

FIG. 6. Purification of HifB–HifD complex and demonstration that antiserum against HifD reacts with purified pili. (*A*) SDS demonstrating purified HifB–HifD complex. Lanes: 1, periplasm from *E. coli* C600/pMMB91 plus pTrc99A without IPTG induction; 2, periplasm from *E. coli* C600/pMMB91 plus pTrc99A induced with IPTG; 3, periplasm from *E. coli* C600/pJS202 plus pGK101 without IPTG induction; 4, periplasm from *E. coli* C600/pJS202 plus pGK101 induced with IPTG; 5, purified HifB–HifD complex; 6, purified HifB. (*B*) Western analysis performed with antiserum against HifD excised from denaturing polyacrylamide gel. Lanes: 1, periplasm from *E. coli* C600/pMMB91 plus pTrc99A without IPTG induction; 2, periplasm from *E. coli* C600/pMMB91 plus pTrc99A induced with IPTG; 3, periplasm from *E. coli* C600/pJS202 plus pGK101 without IPTG induction; 4, periplasm from *E. coli* C600/pJS202 plus pGK101 induced with IPTG; 5, purified pili; 6, purified HifB–HifA complex.

deletion in *hifD* had a similar effect (20). These observations together with our finding that HifD is present at the pilus tip suggest the possibility that this protein functions as an initiator of pilus biogenesis, similar to the PapK and PapF proteins in P pilus tips and the FimF protein in type 1 pilus tips (38–40). HifD contains a signal peptide that is 54 amino acids long and contains a combination of structural features that make it unique. Most striking is the presence of both a signal peptidase II cleavage motif at residues 17–20 and a more typical prokaryotic signal peptide from residues 32–54. It is possible that HifD undergoes multiple processing steps. Whether the amino-terminal processed region has specific functions in addition to being a signal peptide is currently being investigated.

Despite the structural differences between *H. influenzae* pili and P pili, we have demonstrated that *Haemophilus* pilus assembly shares a requirement for a periplasmic chaperone. Based on molecular modeling, it appears that the *H. influenzae* chaperone, designated HifB, is a member of the PapD family of immunoglobulin-like chaperones (6). HifB contains all of the signature features of PapD-like chaperones, including a conserved hydrophobic core and a conserved subunit binding cleft. Data generated in the Pap system have suggested a general model in which the carboxy termini of newly translocated subunits zipper to the G1 β-strand of the chaperone (41). PapD-like chaperones may provide a platform for β-strand zippering, allowing the subunits to achieve their native-like conformations (C. H. Jones and S.J.H., unpublished work). These interactions explain how the chaperone controls pilus assembly by capping and uncapping interactive subunit surfaces. The electron microscopic examination of HifB–HifA complexes revealed the presence of rod-like subassemblies, arguing that the complex is unstable. Whether the surfaces on HifA that participate in the unique packaging interactions remain partially exposed and contribute to the instability of the HifB–HifA complex is unknown.

In summary, *H. influenzae* pili share certain common features with other Gram-negative bacterial pili but are also clearly distinctive. Further investigation of the biogenesis of these structures should contribute to our understanding of protein–protein interactions and provide further insights into the host–parasite relationship.

We thank D. Cutter and R. Roth for expert technical assistance. This work was supported by an American Heart Association Grant-In-Aid and an Infectious Diseases Society of America Young Investigator Award to J.W.S. and by Public Health Service Grant AI29549 to S.J.H.

1. Beachey, E. H. (1981) *J. Infect. Dis.* **143,** 325–345.
2. Hultgren, S. J., Abraham, S., Caparon, M., Falk, P., St. Geme, J. W. & Normark, S. (1993) *Cell* **73,** 887–901.
3. Hung, D. L., Knight, S. & Hultgren S. J. (1996) *EMBO J.* **15,** 3792–3805.
4. Kuehn, M. J., Heuser, J., Normark, S. & Hultgren, S. J. (1992) *Nature (London)* **356,** 252–255.
5. Jones, C. H., Pinkner, J. S., Roth, R., Heuser J., Nicholes, A. V., Abraham, S. N. & Hultgren, S. J. (1995) *Proc. Natl. Acad. Sci. USA* **92,** 2081–2085.
6. Holmgren, A., Kuehn, M. J., Branden, C.-I. & Hultgren, S. J. (1992) *EMBO J.* **11,** 1617–1622.
7. Kuehn, M. J., Normark, S. N. & Hultgren, S. J. (1991) *Proc. Natl. Acad. Sci. USA* **88,** 10586–10590.
8. Dodson, K. W., Jacob-Dubuisson, F., Striker, R. T. & Hultgren, S. J. (1993) *Proc. Natl. Acad. Sci. USA* **90,** 3670–3674.
9. Turk, D. C. (1984) *J. Med Microbiol.* **18,** 1–16.
10. Guerina, N. G., Langermann, S., Clegg, H. W., Kessler, T. W., Goldmann, D. A. & Gilsdorf, J. R. (1982) *J. Infect. Dis.* **146,** 564.
11. Pichichero, M. E., Anderson, P., Loeb, M. & Smith, D. H. (1982) *Lancet* **ii,** 960–962.
12. van Alphen, L., Poole, J. & Overbeeke, M. (1986) *FEMS Microbiol. Lett.* **37,** 69–71.
13. Farley, M. M., Stephens, D. S., Kaplan, S. L. & Mason, E. O., Jr. (1990) *J. Infect. Dis.* **161,** 274–280.
14. Loeb, M. R., Connor, E. & Penney, D. (1988) *Infect. Immun.* **56,** 484–489.
15. Read, R. C., Wilson, R., Rutman, A., Lund, V., Todd, H. C., Brain, A. P. R., Jeffery, P. K. & Cole, P. J. (1991) *J. Infect. Dis.* **163,** 549–558.
16. Weber, A., Harris, K., Lohrke, S., Forney, L. & Smith, A. L. (1991) *Infect. Immun.* **59,** 4724–4728.
17. van Ham, S. M., van Alphen, L, Mooi, F. R. & van Putten, J. P. (1994) *Mol. Microbiol.* **13,** 673–684.
18. van Ham, S. M., van Alphen, L., Mooi, F. R. & van Putten, J. P. M. (1993) *Cell* **73,** 1187–1196.
19. Watson, W. J., Gilsdorf, J. R., Tucci, M. A., McCrea, K. W., Forney, L. J. & Marrs, C. F. (1994) *Infect. Immun.* **62,** 468–475.
20. McCrea, K. W., Watson, W. J., Gilsdorf, J. R. & Marrs, C. F. (1994) *Infect. Immun.* **62,** 4922–4928.
21. Forney, L. J., Marrs, C. F., Bektesh, S. L. & Gilsdorf, J. R. (1991) *Infect. Immun.* **59,** 1991–1996.
22. Sambrook, J., Fritsch, E. F. & Maniatis, T. (1989) *Molecular Cloning: A Laboratory Manual* (Cold Spring Harbor Lab. Press, Plainview, NY), 2nd Ed.
23. Orndorf, P. E. & Falkow, S. (1984) *J. Bacteriol.* **159,** 736–744.
24. Yanisch-Perron, C., Vieira, J. & Messing, J. (1985) *Gene* **33,** 103–119.
25. St. Geme, J. W., III, & Falkow, S. (1991) *Infect. Immun.* **59,** 1325–1333.
26. Heuser, J. (1983) *J. Mol. Biol.* **108,** 401–411.
27. Heuser, J. (1989) *J. Electron Microsc. Tech.* **13,** 244–263.
28. Roberts, J. A., Marklund, B.-I., Ilver, D., Haslam, D., Kaack, M. B., Baskin, G., Louis, M., Mollby, R., Winberg, J. & Normark, S. (1994) *Proc. Natl. Acad. Sci. USA* **91,** 11889–11893.
29. Laemmli, U. K. (1970) *Nature (London)* **227,** 680–685.
30. Donohue-Rolf, A. & Keusch, G. T. (1983) *Infect. Immun.* **39,** 270–274.
31. Slonim, L. N., Pinkner, J. S., Branden, C.-I. & Hultgren, S. J. (1992) *EMBO J.* **11,** 4747–4756.
32. Herriott, R. M., Meyer, E. M. & Vogt, M. (1970) *J. Bacteriol.* **101,** 517–524.
33. Gilsdorf, J. R., McCrea, K. W. & Forney, L. J. (1990) *Infect. Immun.* **58,** 2252–2257.
34. Jones, C. H., Dodson, K. & Hultgren, S. J. (1996) in *Urinary Tract Infections: Molecular Pathogenesis and Clinical Management*, eds. Mobley, H. L. T. & Warren, J. W. (Am. Soc. Microbiol., Washington, DC), pp. 175–219.
35. Bullitt, E. & Makowski, L. (1995) *Nature (London)* **373,** 164–167.
36. Brinton, C. C., Jr. (1965) *Trans. N.Y. Acad. Sci.* **27,** 1003–1165.
37. van Ham, S. M., van Alphen, L, Mooi, F. R. & van Putten, J. P. M. (1995) *Infect. Immun.* **63,** 4883–4889.
38. Jacob-Dubuisson, F., Heuser, J., Dodson, K., Normark, S. & Hultgren, S. (1993) *EMBO J.* **12,** 837–847.
39. Russell, P. W. & Orndorff, P. E. (1992) *J. Bacteriol.* **174,** 5923–5935.
40. Klemm, P. & Christiansen, G. (1987) *Mol. Gen. Genet.* **208,** 439–445.
41. Kuehn, M. J., Ogg, D. J., Kihlberg, J., Slonim, L. N., Flemmer, K., Bergfors, T. & Hultgren, S. J. (1993) *Science* **262,** 1234–1241.
42. Bullitt, E., Jones, C. H., Striker, R., Soto, G., Jacob-Dubuisson, F., Pinkner, J., Wick, M. J., Makowski, L. & Hultgren, S. J. (1996) *Proc. Natl. Acad. Sci. USA* **93,** in press.